



# Ti isotopic evidence for a non-CAI refractory component in the inner Solar System

Samuel Ebert\*, Jan Render, Gregory A. Brennecka, Christoph Burkhardt, Addi Bischoff, Simone Gerber, Thorsten Kleine

Institut für Planetologie, University of Münster, Wilhelm Klemm-Straße 10, 48149 Münster, Germany

## ARTICLE INFO

### Article history:

Received 1 February 2018

Received in revised form 22 June 2018

Accepted 27 June 2018

Available online xxxx

Editor: F. Moynier

### Keywords:

chondrules

Ca,Al-rich inclusion

Na–Al-rich chondrules

Ti isotopes

nucleosynthetic anomalies

disk transport

## ABSTRACT

Understanding the relationships between and among chondritic components of various chondrite groups is of prime importance for deciphering the dynamics of material transport and planetary accretion in the early Solar System. Here we obtain insights into these processes and the reservoirs present by investigating the nucleosynthetic Ti isotopic signatures of individual Ca,Al-rich inclusions (CAIs) and Na–Al-rich chondrules from ordinary and CO chondrites. This specific type of chondrule is of interest as it is thought to have incorporated refractory, CAI-like material as precursors. Our data show that CAIs from ordinary and CO chondrites exhibit  $^{50}\text{Ti}$  excesses that are indistinguishable from CV CAIs, and thus indicate a common source reservoir for refractory inclusions in ordinary, CO, and CV chondrites. Na–Al-rich chondrules from CO chondrites also show  $^{50}\text{Ti}$  excesses, indicating the presence of CAIs from this reservoir in the precursor materials of CO chondrules. In contrast, Na–Al-rich chondrules from ordinary chondrites show no  $^{50}\text{Ti}$  excesses and are indistinguishable from the bulk values for ordinary chondrites. Thus, known CAIs cannot have been the refractory precursor of the Na–Al-rich chondrules in ordinary chondrites. Consequently, within the accretion region of the ordinary chondrites, two different types of refractory components must have existed: (1) a  $^{50}\text{Ti}$ -enriched refractory component that is present as CAIs and either arrived at the accretion region of the ordinary chondrites after chondrule formation, or was only present in insignificant amounts, and (2) another type of refractory material without a  $^{50}\text{Ti}$  excess, which was involved as precursor in the chondrule formation process. Our data thus imply that refractory components with condensation signatures must have formed in at least two isotopically distinct nebular regions. These may be related to non-carbonaceous and carbonaceous source regions, that is, the inner and outer Solar System, divided by the early formation of Jupiter.

© 2018 Elsevier B.V. All rights reserved.

## 1. Introduction

Ca,Al-rich inclusions (CAIs) are regarded as the first solids to have formed in the solar nebula. They are frequently observed in carbonaceous chondrites (up to ~4 vol%; e.g., MacPherson, 2014), but are extremely rare (<<0.1 vol%) in non-carbonaceous chondrites (ordinary, enstatite, and Rumuruti chondrites) (Bischoff and Keil, 1983a, 1983b, 1984; Bischoff et al., 1985; Rout and Bischoff, 2008). On the other hand, chondrules are up to millimeter-sized, silicate-rich, once molten spherules that are the major component of most chondrites, constituting up to 80 vol% of chondritic meteorites (e.g., Weisberg et al., 2006). Even though CAIs and chondrules both formed in the protoplanetary disk and provide pivotal constraints for our understanding of the composition and evolution

of the disk, the genetic relationship between CAIs and chondrules is still a major open question in cosmochemistry.

One possible link between CAIs and chondrules is the existence of Al-rich chondrules, which are believed to have formed from refractory precursors, possibly CAIs, due to their high refractory element content (e.g., Krot and Rubin, 1994; MacPherson and Huss, 2005). A detailed study of the Na-rich variety ( $\text{Al}_2\text{O}_3 > 10 \text{ wt\%}$  and  $\text{Na}_2\text{O} > 4 \text{ wt\%}$ ) of Al-rich chondrules from ordinary, Rumuruti, and CO chondrites (Ebert and Bischoff, 2016) reported highly elevated (up to  $16\times$  CI) rare earth element (REE) abundances. Additionally, Na–Al-rich chondrules have group II, group III, and ultra-refractory REE patterns, similar to those frequently found in CAIs (Mason and Martin, 1977; MacPherson et al., 1988; Davis et al., 2017) and also in some amoeboid olivine aggregates (AOAs) (Grossman et al., 1979). In particular, the group II and ultra-refractory REE patterns are evidence for fractional condensation in the solar nebula and such patterns cannot be created during the

\* Corresponding author.

E-mail address: samuel.ebert@uni-muenster.de (S. Ebert).

chondrule formation process, i.e., melting and crystallization. This combination of elevated refractory and REE abundances, as well as CAI-like REE patterns provide strong evidence that Na–Al-rich chondrules had refractory components like CAIs and AOs as precursors and may represent a link between the first two major types of objects to form in our Solar System (Ebert and Bischoff, 2016).

Because CAIs have pervasive isotopic anomalies (e.g., Dauphas and Schauble, 2016), a powerful way to investigate and test the proposed link between CAIs and chondrules is to compare their isotopic compositions. Only a few elements are well-suited for this task, as the element must be abundant enough in each object to be measured at reasonable precision, and the nucleosynthetic anomalies must be large enough to be distinguished, assuming some mixing with non-refractory materials during chondrule formation. As shown in multiple previous studies, CAIs from CV chondrites (Niederer et al., 1981; Niemeyer and Lugmair, 1981; Leya et al., 2009; Trinquier et al., 2009; Williams et al., 2016; Brennecke et al., 2017; Davis et al., 2017) and CK chondrites (Torrano et al., 2017) exhibit fairly consistent and well-resolved excesses in  $^{50}\text{Ti}$ . Since Ti is present in high abundances in both CAIs and Na–Al-rich chondrules, it is an attractive target for this study. Titanium isotopes are not expected to exchange between the nebular gas and solid phases (Niemeyer, 1988a) and if  $^{50}\text{Ti}$ -enriched material (i.e., CAIs) was involved in chondrule formation,  $^{50}\text{Ti}$  should act as a tracer to constrain the role of CAIs in the chondrule formation process (Niemeyer, 1988a, 1988b; Gerber et al., 2017).

Previous work has shown variations in the  $^{50}\text{Ti}$  signatures of Fe,Mg chondrules in carbonaceous chondrites, revealing admixing of CAI material to chondrule precursors (Niemeyer, 1988a; Gerber et al., 2017). On the contrary, Fe,Mg chondrules of ordinary and enstatite chondrites show no or minor variations in  $^{50}\text{Ti}$  and do not deviate from the  $^{50}\text{Ti}$  composition of their host meteorite (Gerber et al., 2017). From these observations, Gerber et al. (2017) concluded that chondrule formation occurred in distinct regions, and the  $^{50}\text{Ti}$  variations in chondrules from carbonaceous chondrites are caused by admixing  $^{50}\text{Ti}$ -rich material like CAIs in the carbonaceous chondrite (CC) region but not into the enstatite and ordinary chondrite (non-carbonaceous, or NC) region. This contrast between the CC and the NC regions is also visible in bulk meteorites for elements like Cr and Ti (Warren, 2011), as well as Mo (Budde et al., 2016). The separation between the CC and NC regions has been tied to the early formation of Jupiter (Budde et al., 2016; Kruijer et al., 2017), which acted as a physical barrier between the CC and NC regions.

However, if, as is commonly assumed, CAIs formed close to the young Sun (Wood, 2004) and therefore near to the formation region of the NC meteorites of the inner Solar System, it is troubling that CAI-like materials would be primarily admixed to the much more distant CC region where they are chiefly hosted in carbonaceous meteorites. Different models like photophoresis (Wurm et al., 2010), X-winds (Shu et al., 1996), or meridional transport through the disk (Ciesla, 2007) have been proposed to explain the transference of CAIs from close to the Sun to more distal regions of the disk but overall, the general disk dynamics remain poorly understood. Expanding the isotopic dataset of CAIs that is thus far primarily focused on CAIs from carbonaceous chondrites (mainly CV meteorites) may therefore provide key constraints for models of the structure and dynamic evolution of the early circumsolar disk. To this point, only very limited isotopic data exist for CAIs from non-carbonaceous chondrites and these are restricted to O-isotopes and  $^{26}\text{Al}$ – $^{26}\text{Mg}$  systematics (e.g., Hinton and Bischoff, 1984; Russell et al., 1996; McKeegan et al., 1998; Guan et al., 2000a, 2000b; Rout et al., 2009), linking all CAIs to a common formation region and time-frame.

Here we provide the first Ti isotope data for CAIs from ordinary and CO chondrites to constrain the relationship between CAIs present in CC and NC bodies. In addition, we investigate the relationship between CAIs and Na–Al-rich chondrules in the NC and CC reservoirs by analyzing the Ti isotopic composition of Na–Al-rich chondrules from ordinary and CO chondrites.

## 2. Samples and methods

### 2.1. Sample characterization and extraction

All samples investigated in this work were provided by the Institut für Planetologie at the University of Münster. The investigated objects include 15 Na–Al-rich chondrules from five different ordinary chondrites: Northwest Africa (NWA) 6645 (H3-6), Hammadah al Hamra (HaH) 335 (H3), Moorabie (L3.8), Julesburg (L3.6), and Ilafegh 013 (H3.5). Additionally, two Na–Al-rich chondrules and one Na-rich chondrule (NaC-21) from the CO3 meteorite Dar al Gani (DaG) 083 were investigated. Note that chondrule NaC-21 is per definition not a Al-rich chondrule ( $\text{Al}_2\text{O}_3 > 10 \text{ wt}\%$ ) but is enriched in Na. For the CAIs, six inclusions were taken from the ordinary chondrites HaH 335 (H3; two CAIs), Moorabie (L3.8; two CAIs), and Sahara 98175 (L3.5; two CAIs). Additionally, two CAIs were extracted from the CO3 chondrite DaG 083.

Samples were identified and characterized using the JEOL 6610-LV electron microscope (SEM) at the Interdisciplinary Center for Electron Microscopy and Microanalysis (ICEM) at the University of Münster. The attached EDX (Energy Dispersive X-Ray spectroscopy) system (INCA; Oxford Instruments) was used for chemical analyses of the different mineral constituents and the mesostasis at 20 keV. Bulk analyses of the Na–Al-rich chondrules were obtained using the JEOL JXA 8900 Superprobe electron microprobe (EPMA) at ICEM, operated at 15 kV and using a probe current of 15 nA. The bulk chemical analyses of chondrules and mesostasis were performed using defocused beams of variable sizes (20–80  $\mu\text{m}$ ). The investigated objects are from incompletely polished meteorite chips, which were later drilled out for isotopic analysis.

Detailed information about the identification and characterization and about the mineralogy and composition of each sample are given in the electronic supplement. In brief, both CO CAIs are coarse-grained CAIs (one type A, one type B), whereas the ordinary chondrite CAIs all are fine-grained, Fe-spinel rich CAIs (Table 1, 2; Table A1). The Na–Al-rich chondrules are dominated by mesostasis embedding mainly skeletal olivine and pyroxene indicating a fast cooling history. The bulk  $\text{Na}_2\text{O}$  and  $\text{Al}_2\text{O}_3$  concentrations vary from 6.1–13.3 wt% and 8.2–27.8 wt%, respectively (Table A1) and are similar to the Na–Al-rich chondrules described in Ebert and Bischoff (2016).

After petrological characterization, individual samples were extracted from the meteorite chips with a *New Wave Research Micro Mill* following the method of Charlier et al. (2006). Briefly, in order to preserve the sample material during drilling, a piece of cleaned Parafilm with a hole in the center was placed over the sample. A drop of Milli-Q water was placed on top of the hole to capture the sample powder created during the drilling process. Subsequently, the powder/water mixture was removed with a pipette and placed into an acid cleaned Savillex® beaker. As a result of this procedure, and due to the small sample sizes, it was not possible to accurately weigh the samples. Based on the amount of Ti available for isotope measurements and the  $\text{TiO}_2$  content of each CAI, we estimated that typically only 10–30  $\mu\text{g}$  of sample material was extracted.

### 2.2. Titanium purification and isotopic measurements

Following extraction, complete dissolution of each sample was obtained by treating the powdered samples in 2 mL concentrated

**Table 1**  
Main mineral phases and Ti isotopic compositions of measured CAIs.

Sample	Type	Main phases	Size [ $\mu\text{m}$ ]	$f_{\text{CAI}}$	TiO <sub>2</sub> [wt%]	Ti <sub>sol</sub> [ppb]	N <sup>a</sup>	Ca/Ti	$\varepsilon^{50}\text{Ti}_{\text{meas}}$ [ $\pm 2\sigma$ ]	$\varepsilon^{50}\text{Ti}_{\text{corr}}$ [ $\pm 2\sigma$ ]
<b>Moo 1</b>	<b>L3.8</b>	Fe-sp, CaPx, cr-sp, ilm, plag, neph	350 × 150	0.36	1.1	100	2	0.8	2.5 ± 0.7	3.0 ± 0.7
<b>Moo 2</b>	<b>L3.8</b>	Fe-sp, px, fas, ilm, plag,	240 × 260	0.68	3.2	60	1	0.9	6.0 ± 1.3	6.1 ± 1.3
<b>HaH 1</b>	<b>H3</b>	Fe-sp, ilm, Na-rich alt.	130 × 90	0.05	2.0	50	1	1.4	0.7 ± 1.3	2.1 ± 1.5
<b>HaH 2</b>	<b>H3</b>	Fe-sp, CaPx, ilm, Na-rich alt.	190 × 160	0.22	1.0	90	2	0.3	8.0 ± 1.3	11.0 ± 2.0
<b>Sah 041</b>	<b>L3.5</b>	Fe-sp, CaPx, ol, fas, Na-rich alt.	300 × 140	0.27	0.7	60	1	0.9	3.3 ± 1.3	4.9 ± 1.5
<b>Sah 196</b>	<b>L3.5</b>	Fe-sp, CaPx, fas, an	100 × 80	0.03	1.5	30	1	8.4	1.6 ± 1.3	6.7 ± 2.9
<b>DaG 1</b>	<b>CO3</b>	sp, CaPx, mel, an	850 × 750	No cont.	0.6	90	5	0.1	8.9 ± 0.4	n.a.
<b>DaG 2</b>	<b>CO3</b>	sp, mel, pv	900 × 720	No cont.	1.0	90	5	0.1	9.3 ± 0.1	n.a.
<b>EGG2 high</b>		n.a.	n.a.	n.a.	n.a.	300	4	0.1	9.8 ± 0.2	n.a.
		n.a.	n.a.	n.a.	n.a.	110	5	0.1	9.9 ± 0.5	n.a.
<b>BHVO-2</b>		n.a.	n.a.	n.a.	n.a.	270	4	0.1	0.0 ± 0.3	n.a.
<b>Blank</b>		n.a.	n.a.	n.a.	n.a.	15	1	10	0.1 ± 2.6	n.a.

The CAIs DaG 1 and DaG 2 from the CO3 chondrite Dar al Gani 083 were large enough to drill them out without any noticeable host meteorite material and no correction were needed.  $f_{\text{CAI}}$  denotes the fraction of CAI material in each sample. TiO<sub>2</sub> bulk data obtained by microprobe. Ti<sub>sol</sub>: Concentration in Ti-measurement solutions;

<sup>a</sup> Number of analyses on the same sample solution.  $\varepsilon^{50}\text{Ti}_{\text{meas}}$ : measured values;  $\varepsilon^{50}\text{Ti}_{\text{corr}}$ : corrected values; Fe-sp: Fe-rich spinel; CaPx: Ca-rich pyroxene; ilm: ilmenite; cr-sp: Cr-spinel; plag: plagioclase; neph: nepheline; px: pyroxene; fas: fassaite; mel: melilite; ol: olivine; an: anorthite; sp: spinel; pv: perovskite; alt: alteration products; n.a.: not applicable.

**Table 2**  
Ti isotopic compositions of Na–Al-rich chondrules.

Sample	Type	Size [ $\mu\text{m}$ ]	Ti <sub>sol</sub> [ppb]	N <sup>a</sup>	Ca/Ti	$\varepsilon^{50}\text{Ti}_{\text{meas}}$ [ $\pm 2\sigma$ ]
<b>NaC-1</b>	<b>H3-6</b>	240	100	1	0.3	−1.8 ± 0.5
<b>NaC-2</b>	<b>H3-6</b>	460	100	1	0.2	−0.6 ± 0.5
<b>NaC-4</b>	<b>H3</b>	400	100	1	0.5	−0.9 ± 0.5
<b>NaC-5</b>	<b>H3</b>	320	100	1	0.2	−0.4 ± 0.5
<b>NaC-6</b>	<b>L3.8</b>	900 × 650	300	4	0.1	−0.3 ± 0.3
<b>NaC-7</b>	<b>L3.8</b>	250	100	1	0.4	−1.4 ± 0.5
<b>NaC-8</b>	<b>L3.8</b>	300 × 400	100	1	1.4	−1.7 ± 0.5
<b>NaC-9</b>	<b>L3.8</b>	300	100	1	1.2	−1.0 ± 0.5
<b>NaC-10</b>	<b>L3.8</b>	150 × 250	100	1	1.6	−1.3 ± 0.5
<b>NaC-11</b>	<b>L3.8</b>	300 × 220	100	1	2.1	−1.2 ± 0.5
<b>NaC-12</b>	<b>L3.8</b>	900 × 600	300	4	0.1	−0.3 ± 0.4
<b>NaC-13</b>	<b>L3.8</b>	950 × 600	300	4	0.0	−0.3 ± 0.2
<b>NaC-14</b>	<b>L3.6</b>	450	100	1	0.6	−1.5 ± 0.5
<b>NaC-16</b>	<b>H3.5</b>	400 × 500	100	1	0.3	−0.7 ± 0.5
<b>NaC-18</b>	<b>H3.5</b>	600 × 700	300	4	0.1	−0.7 ± 0.3
<b>NaC-20</b>	<b>CO3</b>	350	100	1	1.2	14.5 ± 0.5
<b>NaC-21</b>	<b>CO3</b>	450	100	1	2.6	1.7 ± 0.5
<b>NaC-22</b>	<b>CO3</b>	450	100	1	0.3	13.9 ± 0.5

Ti<sub>sol</sub>: Concentration in Ti-measurement solutions;

<sup>a</sup> Number of analyses on the same sample solution. <sup>50</sup>Ti data were obtained in a measurement session with an external reproducibility of ±0.5 (100 ppb). For comparison: mean OC bulk:  $\varepsilon^{50}\text{Ti} = -0.70$  (Gerber et al., 2017); mean CO bulk:  $\varepsilon^{50}\text{Ti} = 4.07$  (Trinquier et al., 2009); mean CO matrix:  $\varepsilon^{50}\text{Ti} = 2.45$  (Trinquier et al., 2009).

HCl and 100  $\mu\text{L}$  concentrated HF for 14 days on a hotplate at 120 °C, with subsequent treating for 4 days with an additional 2 mL concentrated HNO<sub>3</sub>. All samples were dried and reconstituted in 12M HNO<sub>3</sub> in preparation for Ti separation.

As in our previous Ti isotope study (Gerber et al., 2017), purification of Ti followed the method of Zhang et al. (2011), which employs a two-stage ion-exchange chromatography with pre-cleaned TODGA and Bio-Rad® AG1-X8 resins. After this procedure, the final Ti cuts were dried down and treated with 20  $\mu\text{L}$  H<sub>2</sub>O<sub>2</sub> to remove any organic material from the resins, before being re-dissolved in 0.3M HNO<sub>3</sub>–0.0015M HF for MC-ICP-MS measurements. Procedural blanks from this wet chemistry treatment are typically ~3 ng Ti (Gerber et al., 2017). Additional Ti might, however, have been introduced through incidental inclusion of surrounding bulk chondrite material during the drilling procedure. Therefore, we determined a ‘baseline composition’ of our method by drilling into an area of the OC meteorite Sahara 98175 that did not contain visible CAI material. This baseline composition, including drilling, sample removal, digestion, and column chemistry yielded ~5 ng Ti.

Titanium isotope measurements were performed on the Neptune Plus MC-ICPMS at the University of Münster in combination

with a Cetac Aridus II desolvator. A Saville C-Flow nebulizer with an uptake rate of ~60  $\mu\text{L}/\text{min}$  and a combination of jet sampler and X-skimmer cones resulted in a sensitivity of 135 V/ppm for <sup>48</sup>Ti in medium resolution mode (70 V/ppm for <sup>48</sup>Ti in high resolution mode), while consuming ~350  $\mu\text{L}$  per measurement. Instrumental and natural mass-dependent fractionation was corrected using the exponential law and assuming  $^{49}\text{Ti}/^{47}\text{Ti} = 0.749766$  (Zhang et al., 2011). Results are given in the  $\varepsilon$ -notation as parts-per-ten thousand deviations relative to the Origins Lab OL–Ti standard:

$$\varepsilon^{50}\text{Ti} = 10,000 * \left[ \frac{(^{50}\text{Ti}/^{47}\text{Ti})_{\text{sample}}}{(^{50}\text{Ti}/^{47}\text{Ti})_{\text{standard}}} - 1 \right]$$

Isotope ratios were measured in two separate static measurements: in the first cup configuration all Ti isotopes and monitoring masses 51 and 53 for possible interferences from V and Cr on <sup>50</sup>Ti were measured for 40 cycles of 4.2 s integration time each. Subsequently in a second cup configuration, all Ti isotopes and mass 44 for monitoring possible interferences from Ca on masses <sup>46</sup>Ti and <sup>48</sup>Ti were measured for 20 cycles of 4.2 s integration time each. Due to the relatively low Ti contents (and high Ca) of all samples, we were not able to obtain reliable data for  $\varepsilon^{46}\text{Ti}$  and  $\varepsilon^{48}\text{Ti}$ , and consequently do not report data for these two isotope ratios. By contrast, as there is no direct isobaric interference from Ca on <sup>50</sup>Ti, precise and accurate <sup>50</sup>Ti data could be obtained even for the small amounts of Ti available for each sample (Fig. S1).

As a result of the low total Ti available in many of the samples, the method was tested for low concentration measurements, focused on <sup>50</sup>Ti. Using the setup described above we obtain a  $\varepsilon^{50}\text{Ti}$  reproducibility of ±0.7 (100 ppb), ±0.7 (75 ppb), ±1.3 (50 ppb), ±2.6 (15 ppb) for the OL–Ti standard, as shown in Fig. 1 and given as 2 × standard deviation (2SD). The terrestrial basalt standards BCR-2 and BHVO-2 were measured at concentrations of 50 and 100 ppb Ti, with the obtained values given in Table A2. These combined data were used to estimate the external uncertainty of the Ti isotope measurements for the ordinary chondrite CAIs, which owing to the low amount of Ti recovered from these samples, could only be measured once at relatively low intensity. Further, the external uncertainty on measured  $\varepsilon^{50}\text{Ti}$  for Na–Al-rich chondrules, which all were measured as 100 ppb Ti solutions, is estimated to be ±0.5 (2 SD) (Table 1) based on the reproducibility of the standard during the session in which they were run. For samples that contained sufficient Ti for repeated measurements, the mean and corresponding 95% confidence limits are reported; for those that

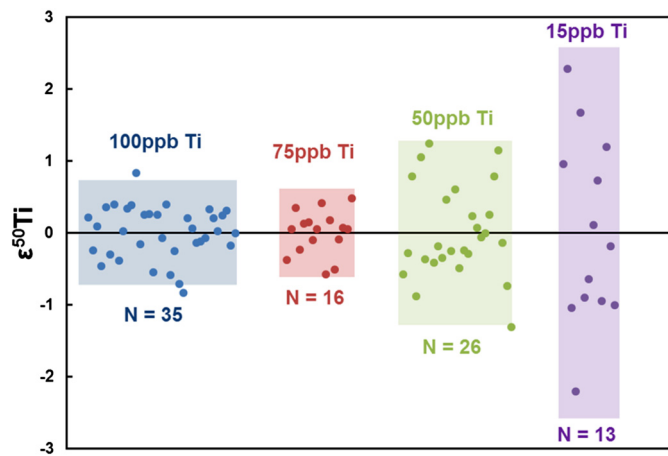


Fig. 1. Reproducibility for  $\epsilon^{50}\text{Ti}$  of bracketing standards with different Ti concentrations.

were measured only once, the 2SD of the standard of that analytical session is used (Table 1).

### 3. Results

#### 3.1. Ca,Al-rich inclusions

The Ti isotopic data of the CAIs analyzed in this study are given in Table 1. The two CAIs from the CO3 chondrite DaG 083 show  $\epsilon^{50}\text{Ti}$  excesses of  $8.9 \pm 0.4$  and  $9.3 \pm 0.1$  (95% conf.,  $N = 5$ ), respectively, consistent with average  $\epsilon^{50}\text{Ti}$  excesses of about 9 observed for many CV CAIs (Niederer et al., 1981; Niemeyer and Lugmair, 1981; Leya et al., 2009; Trinquier et al., 2009; Williams et al., 2016; Brennecka et al., 2017; Davis et al., 2017). Measured  $\epsilon^{50}\text{Ti}$  values for the ordinary chondrite CAIs are lower and more variable, ranging from  $0.7 \pm 1.3$  for CAI HaH 1 to  $8.0 \pm 1.1$  for CAI HaH 2. Since the CAIs from ordinary chondrites were all smaller than the minimum drill size hole of  $>250 \mu\text{m}$  (Fig. 2d), mixing of CAI target material with some amount of the surrounding host meteorite

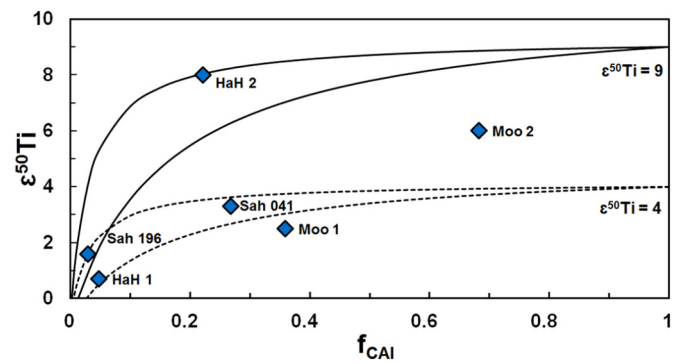


Fig. 3. Measured  $\epsilon^{50}\text{Ti}$  values versus estimated mass fraction of CAI ( $f_{\text{CAI}}$ ) material in the samples. Blue diamonds are measured ordinary chondrite CAI values. The dotted and solid lines are mixing calculations for CAIs with  $\epsilon^{50}\text{Ti} = 4$  (mean value CV chondrites) and with  $\epsilon^{50}\text{Ti} = 9$  (main peak of CV CAIs), respectively and for the host component with  $\epsilon^{50}\text{Ti} = -0.7$ . The  $\text{TiO}_2$  concentrations are in both cases 0.7 and 3.2 wt% for the CAIs and 0.1 wt% for the host material.

during extraction with the micro mill was not avoidable. Note that this is not an issue for the two analyzed CO CAIs, because these were larger than the ordinary chondrite CAIs, and larger than the drill hole size.

The amount of non-CAI material included in each of the ordinary chondrite samples (Table 1) was estimated by comparing the volume of the drill hole with the volume of the CAI, as estimated from the size of each CAI measured in the SEM picture and assuming an ellipsoidal shape for the CAIs. There is a rough correlation between measured  $\epsilon^{50}\text{Ti}$  and the fraction of CAI material in each drilled sample, but the samples do not all plot on mixing lines with a single CAI component of a given  $\epsilon^{50}\text{Ti}$  composition (Fig. 3). Taking the estimated CAI fraction in each sample,  $\epsilon^{50}\text{Ti} = -0.70$  (Gerber et al., 2017) and  $\text{TiO}_2 = 0.1$  wt% for the bulk ordinary chondrite (i.e., the non-CAI material), and the measured Ti isotopic composition and Ti concentration (Table 1) of the CAIs, we obtained contamination-corrected  $\epsilon^{50}\text{Ti}$  for the ordinary chondrite CAIs by mass-balance calculation as follows:

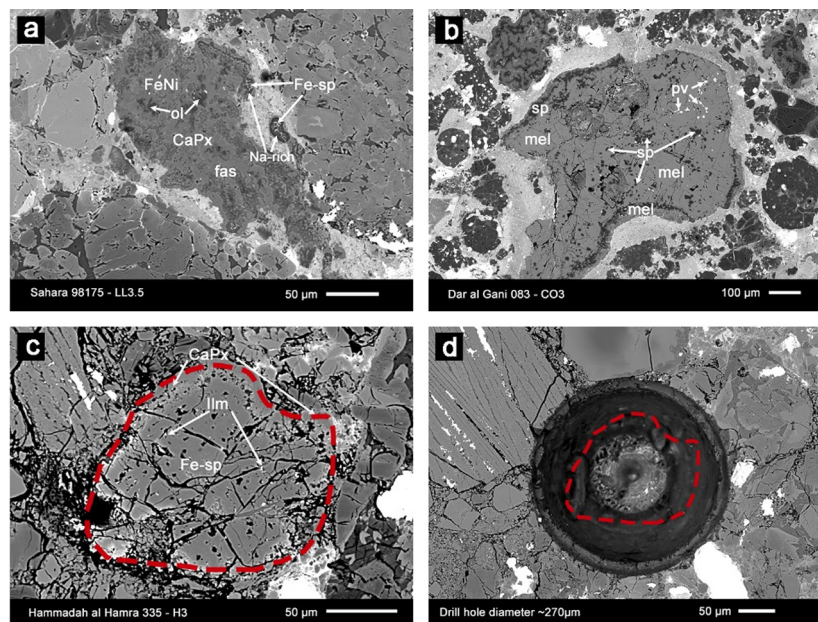
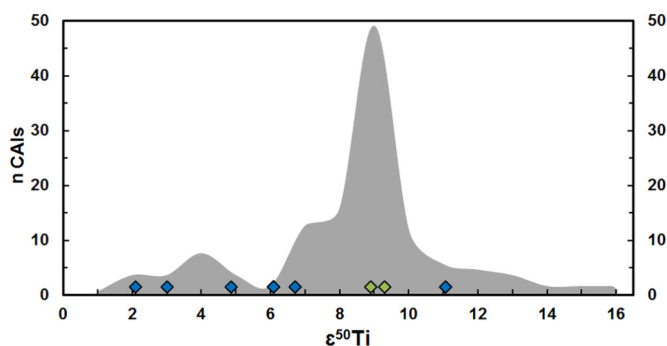


Fig. 2. SEM backscatter images: a) CAI Sah 041 from the LL3.5 meteorite Sahara 98175. b) CAI DaG 2 from the CO3 meteorite Dar al Gani 083. c) CAI HaH 2 from the H3 meteorite Hammadah al Hamra 335. d) HaH 2 drill hole following CAI extraction. The area of the drill hole is larger than the CAI HaH 2 (red dashed line). Note: c) and d) are not shown in the same scale. Fe-sp: Fe-rich spinel; CaPx: Ca-rich pyroxene; ilm: ilmenite; fas: fassaite; mel: melilite; ol: olivine; sp: spinel; pv: perovskite. (For interpretation of the colors in the figure(s), the reader is referred to the web version of this article.)



**Fig. 4.**  $\epsilon^{50}\text{Ti}$  of analyzed ordinary and CO chondrite CAIs in comparison to literature data (gray area) of 101 measured CAIs of CV chondrites (Niemeyer and Lugmair, 1981; Niederer et al., 1981; Niemeyer, 1988b; Leya et al., 2009; Trinquier et al., 2009; Williams et al., 2016; Davis et al., 2017; Brennecka et al., 2017). Of the 101 measured CAIs, 73 have  $^{50}\text{Ti}$  signatures between 7–10 $\epsilon$  with a main peak at  $\sim 9\epsilon$ . The blue diamonds are the six corrected ordinary chondrite CAIs and the green diamonds are the two measured CO CAIs.

$$\epsilon^{50}\text{Ti}_{\text{corr}} = \frac{(f_{\text{CAI}}[\text{Ti}]_{\text{CAI}} + (1 - f_{\text{CAI}})[\text{Ti}]_{\text{host}})\epsilon^{50}\text{Ti}_{\text{meas.}} - (1 - f_{\text{CAI}})[\text{Ti}]_{\text{host}}\epsilon^{50}\text{Ti}_{\text{host}}}{f_{\text{CAI}}[\text{Ti}]_{\text{CAI}}}$$

where  $f_{\text{CAI}}$  denotes the fraction of CAI material in each sample, and  $[\text{Ti}]$  is the Ti concentration in the CAIs and the ordinary chondrite host. This results in corrections ranging from  $\sim 0.1$  (CAI Moo 2) up to  $\sim 5.1$   $\epsilon^{50}\text{Ti}$  (CAI Sah 196) (Table 1). Uncertainties were propagated assuming a 50% uncertainty on the correction, and in the following the given CAI values always refer to the corrected data. Of note, after correction the  $\epsilon^{50}\text{Ti}$  excesses of the ordinary chondrite CAIs are slightly higher, but still show a spread from  $\sim 2$  to  $\sim 11$ . This suggests that this spread is a primary feature of ordinary chondrite CAIs, which is similar to the range of values shown by CAIs from carbonaceous chondrites, although the mean is skewed towards slightly lower anomalies (Fig. 4). However, it cannot be excluded at this stage that the spread in corrected  $\epsilon^{50}\text{Ti}$  values observed for ordinary chondrite CAIs, and in particular the lower values, reflect unaccounted contamination with host meteorite material. This is because estimating the fraction of CAI material in the samples using the measured sizes of the CAIs and the drill holes is inherently uncertain and prone to significant systematic errors. However, regardless of whether or not ordinary chondrite CAIs show a spread in  $\epsilon^{50}\text{Ti}$  compositions, all of them show clear evidence for  $\epsilon^{50}\text{Ti}$  excesses, which are indistinguishable from those observed for CAIs from CV chondrites (Fig. 4).

### 3.2. Na–Al-rich chondrules

The Na–Al-rich chondrules analyzed in this study are all significantly larger than the ordinary chondrite CAIs, and they are also larger than the size of the drill hole used to extract these samples. Thus, unlike for the ordinary chondrite CAIs, contamination of the analyzed Na–Al-rich chondrule samples with material from the chondrite host is not an issue.

The Ti isotope data of the chondrules analyzed in this study are given in Table 2. The three chondrules (NaC-20 to –22) from the CO chondrite DaG 083 all have  $\epsilon^{50}\text{Ti}$  excesses ranging from  $1.7 \pm 0.5$  for NaC-21 to  $\epsilon^{50}\text{Ti} = 14.5 \pm 0.5$  and  $13.9 \pm 0.5$  for NaC-20 and NaC-22, respectively. These excesses are higher than those for the CO CAIs measured here, but are in the range of compositions reported for CV CAIs (e.g., Williams et al., 2016; Davis et al., 2017). By contrast, all 15 investigated Na–Al-rich chondrules from ordinary chondrites (Table 2) show no  $\epsilon^{50}\text{Ti}$  excesses (Fig. 5). Measured  $\epsilon^{50}\text{Ti}$  values range from  $-1.8 \pm 0.5$  to  $-0.3 \pm 0.4$  and, therefore, are indistinguishable from the  $^{50}\text{Ti}$  compositions observed for Fe,Mg chondrules and bulk samples from ordinary chondrites (Gerber et al., 2017).

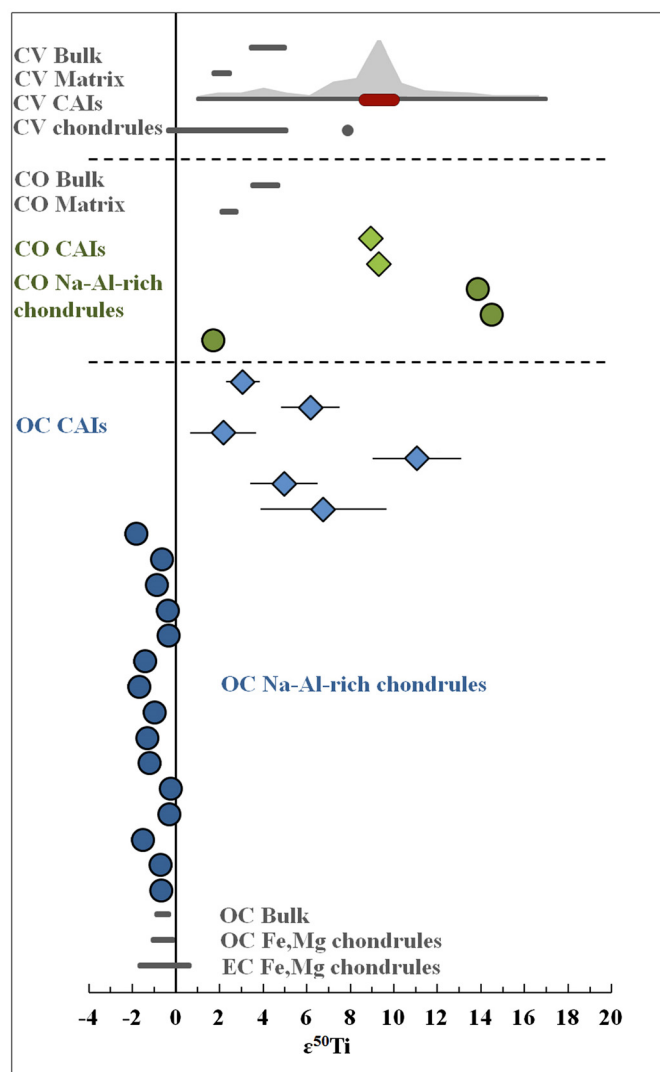


**Fig. 5.** Summary of the new Ti isotope data of chondritic components analyzed in this study (colored symbols) compared to literature data (gray lines: Niemeyer and Lugmair, 1981; Niederer et al., 1981; Niemeyer, 1988b, 1988a; Leya et al., 2008, 2009; Trinquier et al., 2009; Williams et al., 2016; Davis et al., 2017; Gerber et al., 2017; Brennecka et al., 2017). The colored diamonds are CAIs (corrected values for OCs) and the colored circles are the Na–Al-rich chondrules. The light gray area (top) represents the previously measured CV CAIs with their peak around  $\sim 9\epsilon$  (see Fig. 4). Gerber et al. (2017) measured Fe,Mg chondrules (gray line) and one Al-rich chondrule (gray dot).

## 4. Discussion

### 4.1. A common reservoir for CAIs from ordinary and carbonaceous chondrites

CAIs represent a snapshot of the beginning of the Solar System, importantly providing the isotopic composition of its earliest dated reservoir, as well as a fiducial point for disk dynamic models. As such, CAIs have been the focus of numerous scientific studies in the last decades. CAIs are present in all groups of chondritic meteorites, but their abundance and size distribution are widely variable among the groups and links between CAIs of different chondrite groups remain poorly constrained. This knowledge gap stems from the fact that such studies to this point have almost exclusively investigated CAIs from CV chondrites, simply because these CAIs are abundant and sufficiently large for precise isotope analyses, whereas CAIs from non-CV chondrites are comparatively scarce and larger CAIs are missing. Interestingly, some refractory

inclusions from different types of carbonaceous chondrites measured for Ti isotopes include objects such as FUN (fractionated and unidentified nuclear effects) CAIs, PLACs (platy hibonite crystals), hibonite-rich CAIs, or complex CAIs that exhibit large isotopic anomalies with wide ranges in  $\epsilon^{50}\text{Ti}$  of  $-713$  to  $1710$  (Krot et al., 2014 and references therein; Kööp et al., 2016, 2018), respectively. Such objects are thought to have condensed prior to large-scale homogenization of the protoplanetary disk, hence their large nucleosynthetic anomalies, and possibly formed prior to “regular” CAIs (in the following just referred to as CAIs).

Previous works have shown that for CV and CK CAIs a range of  $\epsilon^{50}\text{Ti}$  from  $\sim 2$  to  $16$  with a mean distribution peak around  $9 \epsilon^{50}\text{Ti}$  (Fig. 4) exist (Niemeyer and Lugmair, 1981; Niederer et al., 1981; Niemeyer, 1988b; Leya et al., 2009; Trinquier et al., 2009; Williams et al., 2016; Brennecka et al., 2017; Torrano et al., 2017; Davis et al., 2017). Both CO CAIs analyzed in the present study have  $\epsilon^{50}\text{Ti}$  values of  $\sim 9$ , which are within the range observed for CV CAIs (Figs. 4 and 5). In addition, the CAIs found in ordinary chondrites have  $^{50}\text{Ti}$  excesses that are all within the previously reported range of  $\epsilon^{50}\text{Ti}$  values for CAIs hosted in carbonaceous chondrites.

Given these observations, the Ti isotope data obtained from CAIs in this study lead to the conclusion that CAIs from ordinary chondrites, despite their somewhat different mineralogical composition (Table 1), and CAIs from carbonaceous chondrites (such as CO, CK, and CV) formed from a common isotopic reservoir. This is in agreement with data from other non-carbonaceous chondrite CAIs from O isotopes (McKeegan et al., 1998; Guan et al., 2000a) as well as Al–Mg systematics (Russell et al., 1996; Guan et al., 2000b) that require CAIs from carbonaceous and non-carbonaceous meteorites to be formed within a short window of time.

#### 4.2. CAIs as precursors for Na–Al-rich chondrules in CO chondrites

As  $^{50}\text{Ti}$  excesses are a common feature of CAIs,  $^{50}\text{Ti}$  can be used as a marker of CAI contribution during the chondrule formation process (Niemeyer, 1988a, 1988b; Gerber et al., 2017). For example, chondrules in CV chondrites have been shown to exhibit a wide range of  $\epsilon^{50}\text{Ti}$ , indicating 0–20 wt% of CAI-like refractory material in chondrule precursors of CV chondrites (Gerber et al., 2017). If Na–Al-rich chondrules are indeed the result of admixing a refractory CAI-like component to their precursors, as suggested by previous bulk chemical and mineralogical investigations (Ebert and Bischoff, 2016), then they should be characterized by excess in  $\epsilon^{50}\text{Ti}$ . For example, if the Na–Al-rich chondrules incorporated up to about 50% CAI-like material, as would be required to account for their elevated Ti and REE contents, then they should have an  $^{50}\text{Ti}$  excess of  $\sim 8\text{--}9\epsilon$ . (Fig. 3; assuming that the admixed CAIs and the Fe–Mg component had  $\epsilon^{50}\text{Ti} \sim 9$  and  $\epsilon^{50}\text{Ti} \sim -0.7$ , respectively).

Two of the three investigated chondrules from the CO3 meteorite DaG 083 (NaC-20, NaC-22) have large  $\epsilon^{50}\text{Ti}$  excesses of  $\sim 14$ . Whereas these values are higher than those of the two measured CO CAIs of this study, they are still in the upper range of values reported for CV CAIs (Figs. 4, 5). Such a  $^{50}\text{Ti}$  excess is difficult to envision without refractory components like CAIs in the precursor, because they are the only known components having such elevated  $^{50}\text{Ti}$  signatures. As such, it is likely that nearly all of the Ti in the precursor for both of these Na–Al-rich chondrules derived from CAIs. Conversely, the chondrule NaC-21 has a much smaller excess of only  $\sim 1.7 \epsilon^{50}\text{Ti}$ , which is not higher than the  $\epsilon^{50}\text{Ti}$  of bulk CO3 meteorites, or the matrix from the CO3 chondrite Isna (Trinquier et al., 2009). Thus, for this particular chondrule the Ti isotopic data do not provide clear evidence for the addition of CAI-like material with the typical  $^{50}\text{Ti}$  excesses of around  $\sim 9 \epsilon^{50}\text{Ti}$ . In order to explain the  $\text{TiO}_2$  content of NaC-21 by the addition of a refractory component, this chondrule would need to contain  $\sim 20\%$

of this component. In this case, the  $\epsilon^{50}\text{Ti}$  value of the refractory component cannot have been higher than  $\sim 3$ , because otherwise NaC-21 would contain a larger  $\epsilon^{50}\text{Ti}$  excess than that observed. Note that  $\epsilon^{50}\text{Ti} \sim 3$  is still within the range of Ti isotopic compositions observed for CV CAIs; this value is also in good agreement with the average composition of  $\epsilon^{50}\text{Ti} \sim 4$  inferred by Gerber et al. (2017) for the CAI-like material that has been admixed to CV chondrules. Thus, the Ti isotopic composition of NaC-21, in spite of its lower  $\epsilon^{50}\text{Ti}$  compared to the other two Na–Al-rich chondrules, is also consistent with the admixture of CAI-like material to its precursor.

In summary, the Ti isotopic data for Na–Al-rich chondrules from CO chondrites strongly suggest that CAIs were part of the precursors of these chondrules, and thus are responsible for the enrichment in refractory elements observed for this variety of chondrules. As such, these data together with variable  $^{50}\text{Ti}$  excesses observed for Fe,Mg chondrules from CV chondrites (Gerber et al., 2017) demonstrate that in carbonaceous chondrites, CAIs were present and partially reprocessed during chondrule formation.

#### 4.3. A non-CAI refractory component in the inner Solar System

If chondrules from carbonaceous chondrites, particularly Na–Al-rich chondrules, have been shown to have input from CAIs, it stands to reason that similar chondrules from ordinary and other chondrite groups would have a similar provenance and also include CAI-like precursors with excesses in  $\epsilon^{50}\text{Ti}$ . However, contrary to this expectation, Na–Al-rich chondrules from ordinary chondrites do not show any excesses in  $\epsilon^{50}\text{Ti}$  (Table 2; Fig. 5), but instead have Ti-isotope signatures that are indistinguishable from bulk ordinary chondrites and from Fe,Mg chondrules of ordinary chondrites (Fig. 5). This isotopic similarity exists in spite of the fact that Na–Al-rich chondrules from ordinary chondrites, like the ones from carbonaceous chondrites, exhibit ultra-refractory, group II, and group III REE patterns (Ebert and Bischoff, 2016). Such patterns show that refractory components, formed by condensation in the solar nebula, were part of the precursors of Na–Al-rich chondrules from ordinary chondrites. As such, it is quite unlikely that the Na–Al-rich chondrules from CO chondrites have refractory components as precursors and the Na–Al-rich chondrules from ordinary chondrites, having similar REE-patterns, do not. Yet, although the Na–Al-rich chondrules from CO and ordinary chondrites show similar mineralogy and bulk chemical compositions indicating similar precursor components and a related evolution history, they differ significantly in their Ti isotope systematics.

Mass balance calculations show that  $\sim 30\text{--}80\%$  of refractory CAI-like material in the chondrule precursors is necessary to create the high values for  $\text{TiO}_2$  and  $\text{Al}_2\text{O}_3$  observed for the Na–Al-rich chondrules from ordinary chondrites (Ebert and Bischoff, 2016). If this refractory material were characterized by the  $^{50}\text{Ti}$  excesses ( $\sim 9 \epsilon^{50}\text{Ti}$ ) observed for CAIs, then the Na–Al-rich chondrules would exhibit significant  $^{50}\text{Ti}$  excesses of more than  $\sim 7 \epsilon^{50}\text{Ti}$  (Fig. 3). If instead this refractory material would have had  $\epsilon^{50}\text{Ti} \sim 4$  (i.e., the average composition of CAI-like material admixed to CV chondrules; Gerber et al., 2017), the Na–Al-rich chondrules would still have  $^{50}\text{Ti}$  excesses of more than  $\sim 3 \epsilon^{50}\text{Ti}$  (Fig. 3). However, none of the 15 investigated Na–Al-rich chondrules from ordinary chondrites shows a resolvable  $^{50}\text{Ti}$  excess; instead they all have indistinguishable  $\epsilon^{50}\text{Ti}$  values clustering around a value of about  $-1$ . Thus, unlike for the Na–Al-rich chondrules from CO chondrites, known CAIs with  $\epsilon^{50}\text{Ti}$  excesses cannot be the primary refractory precursor for the Na–Al-rich chondrules from ordinary chondrites. Consequently, a refractory precursor similar in composition to known CAIs, however lacking an excess in  $\epsilon^{50}\text{Ti}$ , is necessary

to account for the isotopic and elemental signatures of Na–Al-rich chondrules from ordinary chondrites.

In summary, in order to explain the different components present in ordinary chondrites, two different types of refractory materials must have been present in the ordinary chondrite formation region: (1) one type of refractory material without a  $^{50}\text{Ti}$  excess which was involved as precursor in the chondrule formation process, and (2) a  $^{50}\text{Ti}$ -enriched refractory component currently present as CAIs that either arrived in the accretion region of the ordinary chondrites after chondrule formation had ceased, or was present in inconsequential amounts. Since no ordinary chondrite CAIs without  $\epsilon^{50}\text{Ti}$  excesses were found, it is possible that all of this non-enriched refractory material was completely reworked during the chondrule formation process and the only traces of this material are preserved in the chemical composition of Na–Al-rich chondrules.

#### 4.4. Distribution of CAIs and other refractory components in the solar nebula

The existence of two different refractory precursors speaks against a common/localized formation region of all refractory components and/or against an isotopically homogeneous formation region. Otherwise all refractory precursors and CAIs should exhibit an excess in  $^{50}\text{Ti}$  and, consequently, this should also be the case for the Na–Al-rich chondrules in ordinary chondrites. A key observation from the Ti isotopic data is that the refractory precursors incorporated into the Na–Al-rich chondrules have the same  $^{50}\text{Ti}$  composition as bulk ordinary chondrites, suggesting strongly that this component formed in the inner solar system. Although the formation mechanism and age of this refractory component remains unclear, its chemical composition and condensation origin inferred from the composition of the Na–Al-rich chondrules indicates that it formed by similar processes as CAIs. Thus, these observations imply that the high temperatures needed for formation of CAI-like material (including CAIs themselves) did not only exist close to the Sun (the presumed formation location of CAIs; e.g. McKeegan et al., 2000), but also at greater heliocentric distances.

Regardless of their formation location, CAIs with  $\epsilon^{50}\text{Ti}$  excesses were unequivocally present early in the carbonaceous chondrite-formation region, as they were mixed in various proportions with non- $\epsilon^{50}\text{Ti}$ -enriched dust to form chondrules (Niemeyer, 1988a; Gerber et al., 2017; this study, Fig. 6a) and eventually cemented into carbonaceous meteorites. A similar scenario likely existed in the inner Solar System (i.e., the formation region of non-carbonaceous chondrites) during chondrule formation; however, the refractory precursors of these chondrules were not  $\epsilon^{50}\text{Ti}$ -enriched. Such a dichotomy between the Ti-isotope signatures of inner and outer Solar System refractory material is consistent with groupings of non-carbonaceous (NC) and carbonaceous (CC) material (Warren, 2011), and may be explained by the separation of the disk into separate reservoirs due to the early formation of Jupiter (Budde et al., 2016; Kruijer et al., 2017). Speculatively, it is therefore possible that the two refractory components, one without  $\epsilon^{50}\text{Ti}$  excess and one with  $\epsilon^{50}\text{Ti}$  excess, represent refractory components formed in the NC and CC regions of the nebula, respectively.

In order to explain the presence of  $\epsilon^{50}\text{Ti}$ -enriched CAIs in ordinary chondrites, some CAIs with  $\epsilon^{50}\text{Ti}$  excesses could have migrated from the carbonaceous chondrite region to the ordinary chondrite region at some point prior to the accretion of ordinary chondrite parent bodies. If indeed the NC and CC regions were separated by Jupiter, this work implies that some small CAIs remained in the inner Solar System following outward transport of material to the outer Solar System, or alternatively (as depicted in Fig. 6), some small CAIs were transported from the CC to the NC region

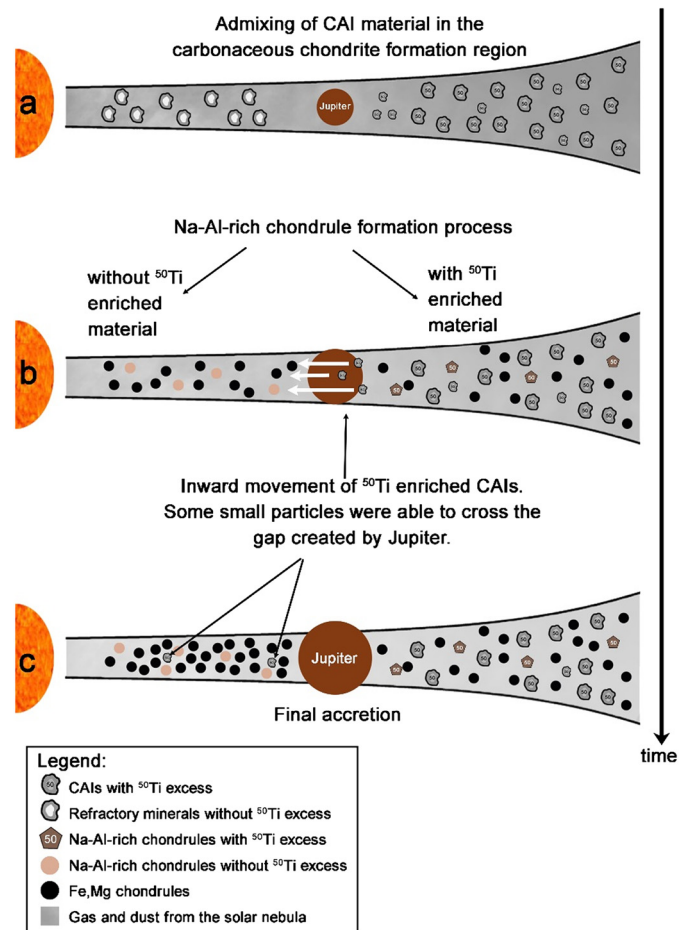


**Fig. 6.** Possible scenario of transportation and distribution of CAIs in the early solar nebula (modified from Gerber et al., 2017) a) Admixing of  $^{50}\text{Ti}$  enriched material with non-enriched material in the carbonaceous chondrite formation region. b) The chondrule formation processes created Fe,Mg chondrules and Na–Al-rich chondrules with  $^{50}\text{Ti}$  excesses in the carbonaceous chondrite region, whereas Fe,Mg chondrules and Na–Al-rich chondrules without  $^{50}\text{Ti}$  excesses were formed in the ordinary chondrite region. c) A limited number of small CAIs with  $^{50}\text{Ti}$  excesses were able to bridge the gap created by Jupiter and were incorporated as isotopically anomalous components in ordinary chondrites.

across the gap created by the formation of Jupiter. As previously suggested, a gap created by a gas giant would not be an impenetrable barrier, and small ( $<150\ \mu\text{m}$ ) particles would be capable of crossing the barrier (Paardekooper and Mellema, 2006). This size constraint would explain why CAIs found in ordinary chondrites are so rare and larger CAIs, like in CV chondrites, are missing, and the size restriction of  $\sim 150\ \mu\text{m}$  is in broad agreement with sizes of the investigated CAIs from this study. Nevertheless, the “permeability” of the gap did not allow widespread mixing of material between the CC and NC regions: only a limited number of small particles were able to bridge the gap and, consequently, the amount of material added was not enough to influence the bulk isotopic composition of the ordinary chondrites. In summary, this scenario explains the isotopic systematics of chondrules and CAIs from both NC and CC reservoirs, and the longstanding observation of why larger CAIs are missing in chondrites accreted in the inner Solar System.

## 5. Conclusions

The Ti isotopic compositions of CAIs and Na–Al-rich chondrules from ordinary and CO chondrites place important constraints on the source reservoirs and transport mechanisms of CAIs. CAIs from

CV, CK, CO, and ordinary chondrites show an excess in  $^{50}\text{Ti}$ , and when paired with existing O-isotope and Al–Mg data, strongly indicate that CAIs from all these meteorite groups formed contemporaneously in a single common region of the solar nebula. All of the Na–Al-rich chondrules from CO chondrites show a  $^{50}\text{Ti}$  excess, which means that they must have incorporated a significant amount of CAIs and/or AOAAs as precursors. Conversely, none of the Na–Al-rich chondrules from ordinary chondrites show any indication of  $^{50}\text{Ti}$  excesses, although, based on their ultra-refractory and group II REE-patterns, refractory precursor components must have been involved in their formation. This can only be explained, if refractory components without  $^{50}\text{Ti}$  excesses were involved as precursors in the formation process of Na–Al-rich chondrules of ordinary chondrites. These unknown refractory precursors formed from materials isotopically indistinguishable from the ordinary chondrite source region, whereas the refractory materials in carbonaceous chondrites have an isotopically distinct signature from the bulk material. The formation process of the refractory materials in the ordinary chondrite source region remains elusive, however our data highlights that high-T condensation must have been active locally in multiple regions of the early solar nebula, including the accretion region of ordinary chondrites. Contrary to current thinking, formation of CAI-like materials, perhaps including CAIs themselves, was not only possible close to the Sun, but also in different regions of the protoplanetary disk.

### Acknowledgements

We thank Knut Metzler and Markus Patzek for fruitful discussions, Jasper Berndt-Gerdes and Beate Schmitte for analytical support, Ulla Heitmann for meteorite preparation, Erik Scherer for introduction and use of the micro mill, and Celeste Brennecke for writing support. Furthermore, we thank Andrew Davis and an anonymous reviewer who provided useful reviews of the manuscript as well as Frédéric Moynier for careful editorial handling. This work was partly supported by the German Research Foundation (DFG) within the Collaborative Research Center/Transregio TRR 170 and the Research Priority Program SPP 1385 (KL 1857/4), as well as a Sofja Kovalevskaja award from Alexander von Humboldt Foundation (G.A.B.). This is TRR 170 publication No. 36.

### Appendix A. Supplementary material

Supplementary material related to this article can be found online at <https://doi.org/10.1016/j.epsl.2018.06.040>.

### References

- Bischoff, A., Keil, K., 1983a. Ca–Al-rich chondrules and inclusions in ordinary chondrites. *Nature* 303, 588–592. <https://doi.org/10.1038/303588a0>.
- Bischoff, A., Keil, K., 1983b. Catalog of Al-Rich Chondrules, Inclusions and Fragments in Ordinary Chondrites. Special Publication No. 22. UNM, Institute of Meteoritics, Albuquerque, pp. 1–33.
- Bischoff, A., Keil, K., 1984. Al-rich objects in ordinary chondrites: related origin of carbonaceous and ordinary chondrites and their constituents. *Geochim. Cosmochim. Acta* 48, 693–709. [https://doi.org/10.1016/0016-7037\(84\)90096-6](https://doi.org/10.1016/0016-7037(84)90096-6).
- Bischoff, A., Keil, K., Stöffler, D., 1985. Perovskite-hibonite-spinel-bearing inclusions and Al-rich chondrules and fragments in enstatite chondrites. *Chem. Erde* 44, 97–106.
- Brennecke, G.A., Burkhardt, C., Kruijjer, T.S., Kleine, T., 2017. Towards understanding the source of nucleosynthetic anomalies in refractory inclusions. *Lunar Planet. Sci. XLVIII*, #1619.
- Budde, G., Burkhardt, C., Brennecke, G.A., Fischer-Gödde, M., Kruijjer, T.S., Kleine, T., 2016. Molybdenum isotopic evidence for the origin of chondrules and a distinct genetic heritage of carbonaceous and non-carbonaceous meteorites. *Earth Planet. Sci. Lett.* 454, 293–303. <https://doi.org/10.1016/j.epsl.2016.09.020>.
- Charlier, B.L.A., Ginibre, C., Morgan, D., Nowell, G.M., Pearson, D.G., Davidson, J.P., Ottley, C.J., 2006. Methods for the microsampling and high-precision analysis of strontium and rubidium isotopes at single crystal scale for petrological and geochronological applications. *Chem. Geol.* 232, 114–133. <https://doi.org/10.1016/j.chemgeo.2006.02.015>.
- Ciesla, F.J., 2007. Outward transport of high-temperature materials around the mid-plane of the solar nebula. *Science* 318, 613–615. <https://doi.org/10.1126/science.1147273>.
- Davis, A.M., Zhang, J., Greber, N.D., Hu, J., Tissot, F.J.H., Dauphas, N., 2017. Titanium isotopes and rare earth patterns in CAIs: evidence for thermal processing and gas-dust decoupling in the protoplanetary disk. *Geochim. Cosmochim. Acta*. <https://doi.org/10.1016/j.gca.2017.07.032>. In press.
- Dauphas, N., Schauble, E.A., 2016. Mass fractionation laws, mass-independent effects, and isotopic anomalies. *Annu. Rev. Earth Planet. Sci.* 44, 709–783. <https://doi.org/10.1146/annurev-earth-060115-012157>.
- Ebert, S., Bischoff, A., 2016. Genetic relationship between Na-rich chondrules and Ca,Al-rich inclusions? – Formation of Na-rich chondrules by melting of refractory and volatile precursors in the solar nebula. *Geochim. Cosmochim. Acta* 177, 182–204. <https://doi.org/10.1016/j.gca.2016.01.014>.
- Gerber, S., Burkhardt, C., Budde, G., Metzler, K., Kleine, T., 2017. Mixing and transport of dust in the early solar nebula as inferred from titanium isotope variations among chondrules. *Astrophys. J. Lett.* 841, L17. <https://doi.org/10.3847/2041-8213/aa72a2>.
- Grossman, L., Ganapathy, R., Methot, R.L., Davis, A.M., 1979. Trace elements in the Allende Meteorite-IV. Amoeboid olivine aggregates. *Geochim. Cosmochim. Acta* 43, 817–829.
- Guan, Y., McKeegan, K.D., MacPherson, G.J., 2000a. Oxygen isotopes in calcium-aluminum-rich inclusions from enstatite chondrites: new evidence for a single CAI source in the solar nebula. *Earth Planet. Sci. Lett.* 181, 271–277. [https://doi.org/10.1016/S0012-821X\(00\)00218-1](https://doi.org/10.1016/S0012-821X(00)00218-1).
- Guan, Y., Huss, G.R., MacPherson, G.J., Wasserburg, G.J., 2000b. Calcium–aluminum-rich inclusions from enstatite chondrites: indigenous or foreign? *Science* 289, 1330–1333. <https://doi.org/10.1126/science.289.5483.1330>.
- Hinton, R.W., Bischoff, A., 1984. Ion microprobe magnesium isotope analysis of plagioclase and hibonite from ordinary chondrites. *Nature* 308 (5955), 169–172. <https://doi.org/10.1038/308169a0>.
- Kööp, L., Davis, A.M., Nakashima, D., Park, C., Krot, A.N., Nagashima, K., Tenner, T.J., Heck, P.R., Kita, N.T., 2016. A link between oxygen, calcium and titanium isotopes in  $^{26}\text{Al}$ -poor hibonite-rich CAIs from Murchison and implications for the heterogeneity of dust reservoirs in the solar nebula. *Geochim. Cosmochim. Acta* 189, 70–95. <https://doi.org/10.1016/j.gca.2016.05.014>.
- Kööp, L., Davis, A.M., Krot, A.N., Nagashima, K., Simon, S.B., 2018. Calcium and titanium isotopes in refractory inclusions from CM, CO, and CR chondrites. *Earth Planet. Sci. Lett.* 489, 179–190. <https://doi.org/10.1016/j.epsl.2018.02.029>.
- Krot, A.N., Rubin, A.E., 1994. Glass-rich chondrules in ordinary chondrites. *Meteorit. Planet. Sci.* 29, 697–707. <https://doi.org/10.1111/j.1945-5100.1994.tb00787.x>.
- Krot, A.N., Nagashima, K., Wasserburg, G.J., Huss, G.R., Papanastassiou, D., Davis, A.M., Hutcheon, I.D., Bizzarro, M., 2014. Calcium–aluminum-rich inclusions with fractionation and unknown nuclear effects (FUN CAIs): I. Mineralogy, petrology, and oxygen isotopic compositions. *Geochim. Cosmochim. Acta* 145, 206–247. <https://doi.org/10.1016/j.gca.2014.09.027>.
- Kruijjer, T.S., Burkhardt, C., Budde, G., Kleine, T., 2017. Age of Jupiter inferred from the distinct genetics and formation times of meteorites. *Proc. Natl. Acad. Sci.* 144, 6712–6716. <https://doi.org/10.1073/pnas.1704461114>.
- Leya, I., Schönbächler, M., Wiechert, U., Krähenbühl, U., Halliday, A.N., 2008. Titanium isotopes and the radial heterogeneity of the solar system. *Earth Planet. Sci. Lett.* 266, 233–244. <https://doi.org/10.1016/j.epsl.2007.10.017>.
- Leya, I., Schönbächler, M., Krähenbühl, U., Halliday, A.N., 2009. New titanium isotope data for Allende and Efremovka CAIs. *Astrophys. J.* 702, 1118–1126. <https://doi.org/10.1088/0004-637X/702/2/1118>.
- MacPherson, G.J., 2014. Calcium–aluminum-rich inclusions in chondritic meteorites. In: Davis, A.M., Holland, H.D., Turekian, K.K. (Eds.), *Meteorites and Cosmochemical Processes, Treatise on Geochemistry*, vol. 1. Elsevier, Oxford, pp. 139–179.
- MacPherson, G.J., Huss, G.R., 2005. Petrogenesis of Al-rich chondrules: evidence from bulk compositions and phase equilibria. *Geochim. Cosmochim. Acta* 69, 3099–3127. <https://doi.org/10.1016/j.gca.2004.12.022>.
- MacPherson, G.J., Wark, D.A., Armstrong, J.T., 1988. Primitive material surviving in chondrites: refractory inclusions. In: Kerridge, J.F., Matthews, M.S. (Eds.), *Meteorites and the Early Solar System*. Univ. Arizona Press, Tucson, pp. 746–807.
- Mason, B., Martin, P.M., 1977. Geochemical differences among components of the Allende meteorite. *Smithson. Contrib. Earth Sci.* 19, 84–95.
- McKeegan, K.D., Leshin, L.A., Russell, S.S., MacPherson, G.J., 1998. Oxygen isotopic abundances in calcium–aluminum-rich inclusions from ordinary chondrites: implications for nebular heterogeneity. *Science* 280, 414–418. <https://doi.org/10.1126/science.280.5362.414>.
- McKeegan, K.D., Chaussidon, M., Robert, F., 2000. Incorporation of short-lived  $^{10}\text{Be}$  in a calcium–aluminum-rich inclusion from the Allende meteorite. *Science* 289, 1334–1337. <https://doi.org/10.1126/science.289.5483.1334>.
- Niederer, F.R., Papanastassiou, D.A., Wasserburg, G.J., 1981. The isotopic composition of titanium in the Allende and Leoville meteorites. *Geochim. Cosmochim. Acta* 45, 1017–1031. [https://doi.org/10.1016/0016-7037\(81\)90128-9](https://doi.org/10.1016/0016-7037(81)90128-9).
- Niemeyer, S., 1988a. Titanium isotopic anomalies in chondrules from carbonaceous chondrites. *Geochim. Cosmochim. Acta* 52, 309–318. [https://doi.org/10.1016/0016-7037\(88\)90086-5](https://doi.org/10.1016/0016-7037(88)90086-5).

- Niemeyer, S., 1988b. Isotopic diversity in nebular dust: the distribution of Ti isotopic anomalies in carbonaceous chondrites. *Geochim. Cosmochim. Acta* 52, 2941–2954. [https://doi.org/10.1016/0016-7037\(88\)90159-7](https://doi.org/10.1016/0016-7037(88)90159-7).
- Niemeyer, S., Lugmair, G.W., 1981. Ubiquitous isotopic anomalies in Ti from normal Allende inclusions. *Earth Planet. Sci. Lett.* 53, 211–225. [https://doi.org/10.1016/0012-821X\(81\)90155-2](https://doi.org/10.1016/0012-821X(81)90155-2).
- Paardekooper, S.-J., Mellema, G., 2006. Dust flows in gas disks in the presence of embedded planets. *Astron. Astrophys.* 453, 1129–1140. <https://doi.org/10.1051/0004-6361:20054449>.
- Rout, S.S., Bischoff, A., 2008. Ca,Al-rich inclusions in Rumuruti (R) chondrites. *Meteorit. Planet. Sci.* 43, 1439–1464. <https://doi.org/10.1111/j.1945-5100.2008.tb01020.x>.
- Rout, S.S., Bischoff, A., Nagashima, K., Krot, A.N., Huss, G.R., Keil, K., 2009. Oxygen- and magnesium-isotope compositions of calcium–aluminum-rich inclusions from Rumuruti (R) chondrites. *Geochim. Cosmochim. Acta* 73, 4264–4287. <https://doi.org/10.1016/j.gca.2009.04.006>.
- Russell, S.S., Srinivasan, G., Huss, G.R., Wasserburg, G.J., MacPherson, G.J., 1996. Evidence for widespread  $^{26}\text{Al}$  in the solar nebula and constraints for nebula time scales. *Science* 273, 757–762. <https://doi.org/10.1126/science.273.5276.757>.
- Shu, F.H., Shang, H., Lee, T., 1996. Toward an astrophysical theory of chondrites. *Science* 271, 1545–1552. <https://doi.org/10.1126/science.271.5255.1545>.
- Torrano, Z.A., Rai, V.K., Wadhwa, M., 2017. Magnesium, titanium and chromium isotope compositions of refractory inclusions from several CV3 and CK3 chondrites: implications for nebular heterogeneity. *Lunar Planet. Sci. XLVIII*, #3045.
- Trinquier, A., Elliott, T., Ulfbeck, D., Coath, C., Krot, A.N., Bizzarro, M., 2009. Origin of nucleosynthetic isotope heterogeneity in the solar protoplanetary disk. *Science* 324, 374–376. <https://doi.org/10.1126/science.1168221>.
- Warren, P.H., 2011. Stable-isotopic anomalies and the accretionary assemblage of the Earth and Mars: a subordinate role for carbonaceous chondrites. *Earth Planet. Sci. Lett.* 311, 93–100. <https://doi.org/10.1016/j.epsl.2011.08.047>.
- Weisberg, M.K., McCoy, T.J., Krot, A.N., 2006. Systematics and evaluation of meteorite classification. In: Lauretta, D.S., McSween Jr., H.Y. (Eds.), *Meteorites and the Early Solar System II*. University of Arizona Press, Tucson, pp. 19–52.
- Williams, C.D., Janney, P.E., Hines, R.R., Wadhwa, M., 2016. Precise titanium isotope compositions of refractory inclusions in the Allende CV3 chondrite by LA-MC-ICPMS. *Chem. Geol.* 436, 1–10. <https://doi.org/10.1016/j.chemgeo.2016.04.021>.
- Wood, J.A., 2004. Formation of chondritic refractory inclusions: the astrophysical setting. *Geochim. Cosmochim. Acta* 68, 4007–4021. <https://doi.org/10.1016/j.gca.2004.04.003>.
- Wurm, G., Teiser, J., Bischoff, A., Haack, H., Roszjar, J., 2010. Experiments on the photophoretic motion of chondrules and dust aggregates – indications for the transport of matter in protoplanetary disk. *Icarus* 208, 482–491. <https://doi.org/10.1016/j.icarus.2010.01.033>.
- Zhang, J., Dauphas, N., Davis, A.M., Pourmand, A., 2011. A new method for MC-ICPMS measurement of titanium isotopic composition: identification of correlated isotope anomalies in meteorites. *J. Anal. At. Spectrom.* 26, 2197–2205. <https://doi.org/10.1039/C1JA10181A>.